

# **CHAPTER – V**

**Ruthenium (II) Complexes of azo ligands  
having O, N, S donor system: Isolation and  
characterization**

## CHAPTER - V

### **Ruthenium (II) Complexes of azo ligands having O,N,S donor system: Isolation and characterization**

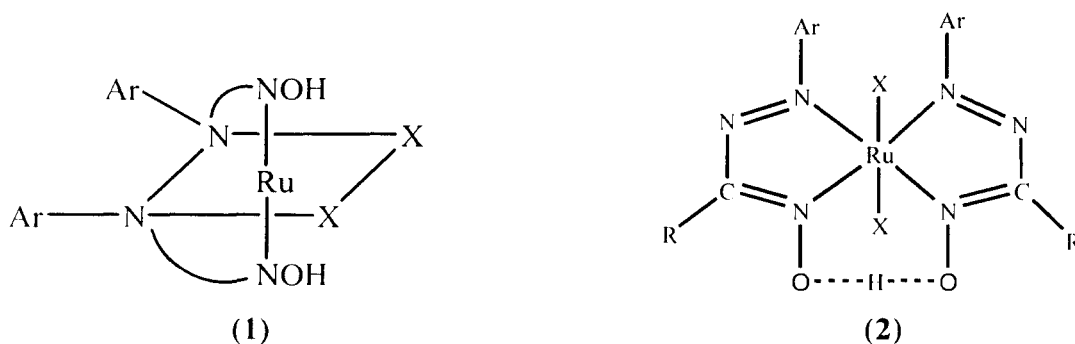
#### **Abstract**

Reaction of 2-hydroxy-1-(2'-alkylthiophenylazo)naphthalenes and 1-hydroxy-2-(2'-alkylthiophenylazo)naphthalenes (HL) where H stands for the dissociable proton, and alkyl groups are CH<sub>3</sub>, C<sub>2</sub>H<sub>5</sub>, C<sub>3</sub>H<sub>7</sub>, C<sub>4</sub>H<sub>9</sub> and CH<sub>2</sub>Ph with [Ru(PPh<sub>3</sub>)<sub>2</sub>Cl<sub>2</sub>] in refluxing dry ethanol medium leads to formation of complexes of the type [Ru(L)(PPh<sub>3</sub>)<sub>2</sub>Cl]. In contrast, the diazene ligands (HL) reacts with RuCl<sub>3</sub> · xH<sub>2</sub>O in boiling ethanol and form ruthenium(II) complexes of the type [Ru<sup>II</sup>(L)<sub>2</sub>]. All the ruthenium compounds have been isolated in pure form and characterized by micro analytical and spectroscopic (IR, electronic, NMR) data. X-ray crystallographic analysis of one the representative member of [Ru<sup>II</sup>(L)<sub>2</sub>] series has been reported. The complexes are diamagnetic (low spin d<sup>6</sup>, S=0). These complexes show intense MLCT transitions in the visible region and characteristic spectral properties.

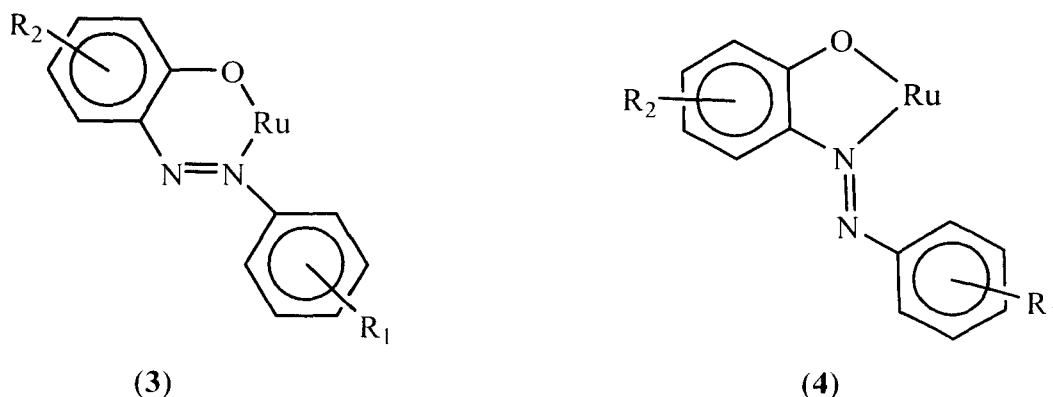
## V. 1 Introduction

The interest in the chemistry of ruthenium is primarily due to the versatile electron-transfer properties exhibited by its complexes [1]. The coordination environment around ruthenium often plays important roles in stabilizing different oxidation states and hence dictates the redox properties of the complexes [2]. Ruthenium complexes of azo ligands are particularly interesting in this regard [2a]. The azo (-N=N-) functions due to their pronounced  $\pi$ -acid character, stabilize the lower metal oxidation states, *viz.* Ru(II) and Ru(III) [3].

Chakravorty *et al.* thoroughly examined the reactivity of ruthenium towards (aryloxo) oximes and synthesized both Ru(II) and Ru(III) complexes of (aryloxo)oximes (1 & 2) [4].

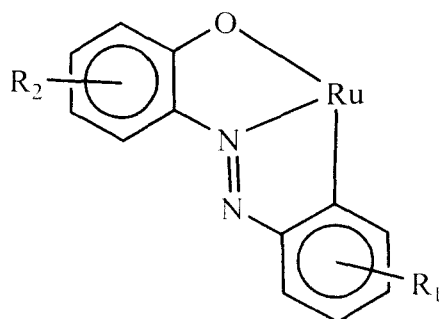


The 2-(aryloxo) phenols, on the other hand, are known to bind to ruthenium usually as bidentate N,O-donors *via* dissociation of the phenolic proton, forming a six-membered chelate ring (3) [5]. However, 2-(aryloxo)phenols can also coordinate ruthenium as bidentate N,O donors forming a stable five-membered chelate ring (4) [6].



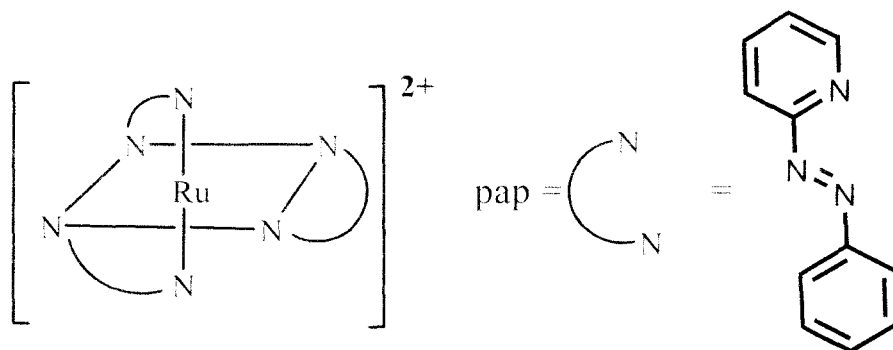
In the solid state the pendent phenyl ring in the aryloxo fragment in (4) is observed to remain almost orthogonal to the plane of the chelate ring. In view of the possible rotation

of the phenyl ring around the C-N bond in the solution phase and particularly in view of the resulting closeness of the phenyl ring to the metal center when it becomes coplanar with the chelate ring, C-H activation at the ortho position of the phenyl [5] has been found to occur [7].



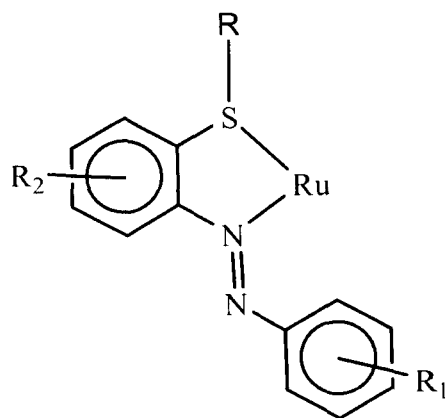
(5)

Ruthenium complexes of 2-(Arylazo)pyridines (6) have received considerable interest, particularly because of interesting electronic and redox properties [8]. 2-(Arylazo)pyridines are excellent  $\pi$ -acceptors and their complexes with electron rich metal centres such as Ru(II) are characterized by strong metal-to-ligand back-bonding [9].

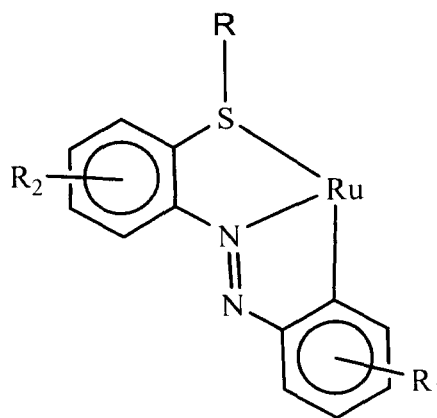


(6)

In case of binding of ruthenium by a group of N(azo), S(thioether) ligands viz. 2-(arylazo)phenyl thioethers where two pi acceptor sites-azo and sulphur are involved, two modes of chelation, viz. N,S (7) and C,N,S (8 via ortho metallation) are observed with a preponderance of the latter [10].

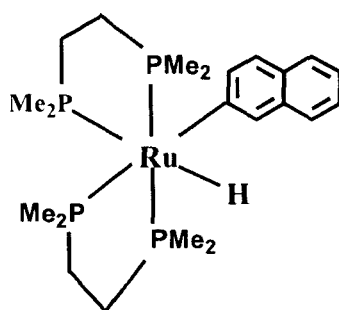


(7)



(8)

On the other hand, Complex of ruthenium with naphthyl ring is hitherto unknown but Chatt and Davidson reported the synthesis of divalent ruthenium organometallate  $[\text{Ru}(\text{dmpe})_2(\text{H})(\text{C}_{10}\text{OH}_7)]$  by reacting *trans* -  $[\text{Ru}(\text{dmpe})_2\text{Cl}_2]$  with  $\text{Na}(\text{C}_{10}\text{H}_7)$  [11]. The crystal structure of  $[\text{Ru}(\text{dmpe})_2(\text{H})(\text{C}_{10}\text{OH}_7)]$  (9) was determined by Gregory *et al.*[12]



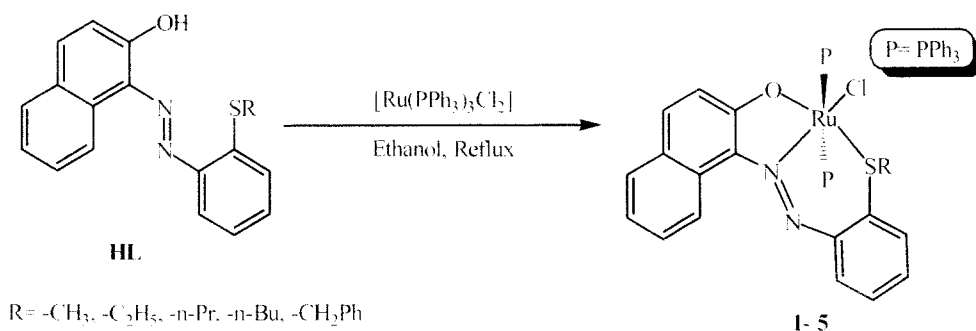
(9)

The main objective of our work is to explore the reactivity of the terdentate monoanionic azo-ligands ( $\text{HL}^{1-10}$ ) towards ruthenium. Both ruthenium(II) and ruthenium(III) starting materials have been used to synthesize novel azo-ruthenium complexes. Syntheses and characterization of these azo-ruthenium(II) complexes together with their electronic features have been described. TD-DFT calculations have been performed to gain insight into the interesting spectroscopic properties of the ruthenium(II) complexes.

## V. 2 Results and Discussion

### V. 2. 1 Syntheses

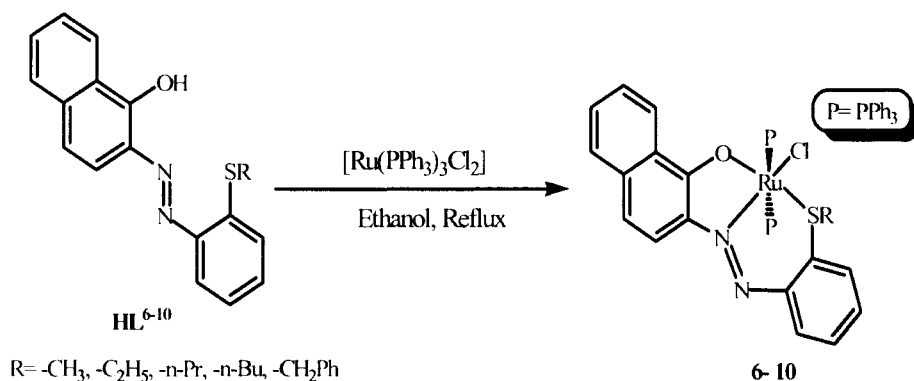
The terdentate monoanionic ligands ( $HL^1$ - $HL^5$ ) reacts smoothly with  $[Ru(PPh_3)_3Cl_2]$  in ethanol under dinitrogen atmosphere and afford a deep green mixture in 8h. The crude mass, so obtained, was subjected to thin layer chromatographic separation on silica to yield pale green product (**1 – 5**) (Scheme V.1).



**Scheme V.1.** Reactions of  $[Ru(PPh_3)_3Cl]$  with the azo-ligands ( $HL^1$ - $HL^5$ ).

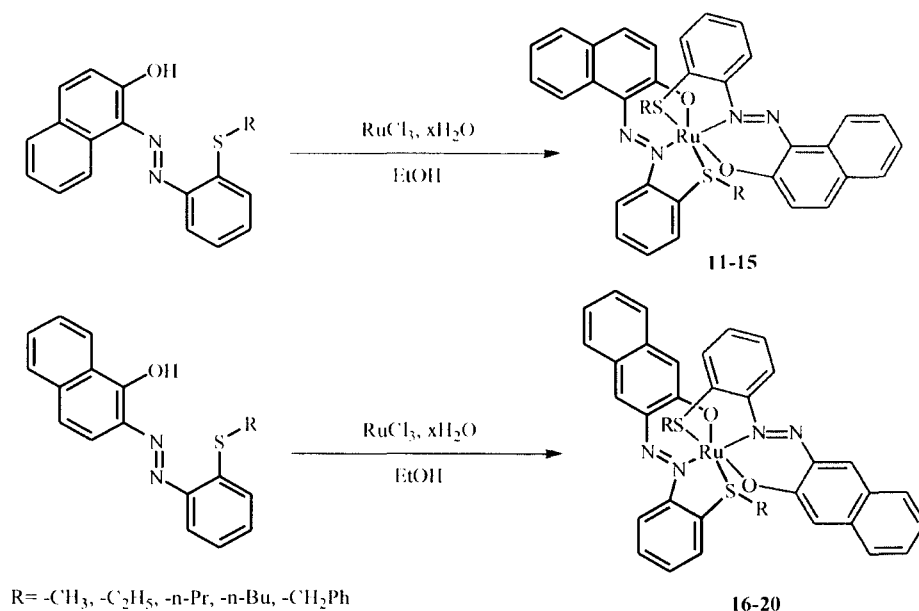
Magnetic susceptibility measurements indicated the compounds to be diamagnetic. Elementary analysis and spectroscopic data clearly showed the compositions to be  $[Ru(L)(PPh_3)_2Cl]$ . Formation of Ru(II) complexes was further confirmed by the fact that these complexes afforded non-conducting solutions in polar media. The complexes have been characterized by their  $^1H$  NMR spectra that clearly show the presence of alkyl groups coordinated to thioether S. All other signals lie in aromatic region.

The second set of ligands, *viz.*, 1-hydroxy-2-(2'-alkylthiophenylazo)naphthalenes ( $HL^6$ - $HL^{10}$ ) was found to react in a similar fashion with  $[Ru(PPh_3)_3Cl_2]$  (Scheme V.2). Thus, the reaction between the ligands ( $HL^6$ - $HL^{10}$ ) and  $[Ru(PPh_3)_2Cl_2]$  in refluxing dry ethanol under dinitrogen atmosphere for 8 h, which also afforded a deep green mixture, which on separation and isolation gave again a deep green compounds. The preliminary characterizations (microanalysis IR,  $^1HNMR$ ) of the complex shows the ligands are coordinated to ruthenium as a monoanionic tridentate O, N, S donor. Two triphenylphosphines and a chloride are also coordinated to the metal centre.



**Scheme V.2.** Reactions of  $[\text{Ru}(\text{PPh}_3)_3\text{Cl}_2]$  with the azo-ligands ( $\text{HL}^6$ - $\text{HL}^{10}$ ).

Formation of diamagnetic ruthenium(II) complexes in the above two cases encourage us to extend our study to explore the chemistry of the diazene derivatives (HL) towards a higher valent ruthenium starting material. Reactions between  $\text{RuCl}_3$  and HL proceed smoothly in boiling ethanol under nitrogen atmosphere. On cooling, pink coloured crystals of the composition  $[\text{Ru}(\text{L})_2]$  deposited (Scheme V.3).



**Scheme V.3.** Reactions of  $\text{RuCl}_3 \cdot x\text{H}_2\text{O}$  with the azo-ligands ( $\text{HL}^1$ - $\text{HL}^{10}$ ).

X-ray structure solution of the complex  $[\text{Ru}(\text{L}^1)_2]$  (**11**) reconfirms the formulation as well as the geometry (Figure V.1). The crystal parameters are compiled in Table V.1, and the selected bond parameters are listed in Table V.2. The central ruthenium(II) in **11** is coordinated by two azo nitrogens, two oxygens and two thioether S atoms arranged in an irregular octahedron. The coordinated azo nitrogen atoms are mutually *trans* to each other while the oxygen atoms are *cis* to each other. This gives the immediate coordination shell approximate  $C_2$  symmetry, with the twofold axis bisecting O(1)-

Ru(1)-O(2) fragment. Similar arrangement of ligands has been reported in case of ruthenium(II) complexes of arylazooximes [4]. The two azo N-N distances, *viz.* N1-N2 and N3-N4 are 1.270 and 1.286 Å respectively and correspond to  $-N=N-$  descriptions. The Ru-N(azo) lengths, 2.004 and 2.018 Å, are nearly equal. The  $[RuL^1]$  motifs are essentially planar and mutually perpendicular to each other (Figure V.2). The relative shorter Ru-N(azo) lengths and longer N-N bond lengths can be correlated to the presence of substantial Ru ( $t_2$ )  $\rightarrow$  azo ( $\pi^*$ ) back-bonding.

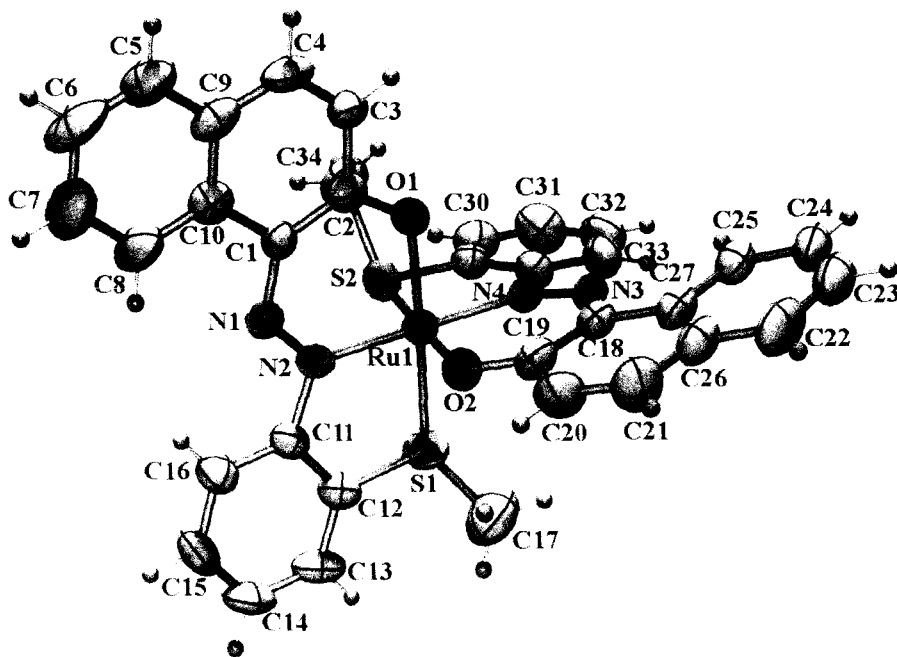


Figure V.1. ORTEP view of the complex 11. Thermal ellipsoids are drawn at 50% probability.

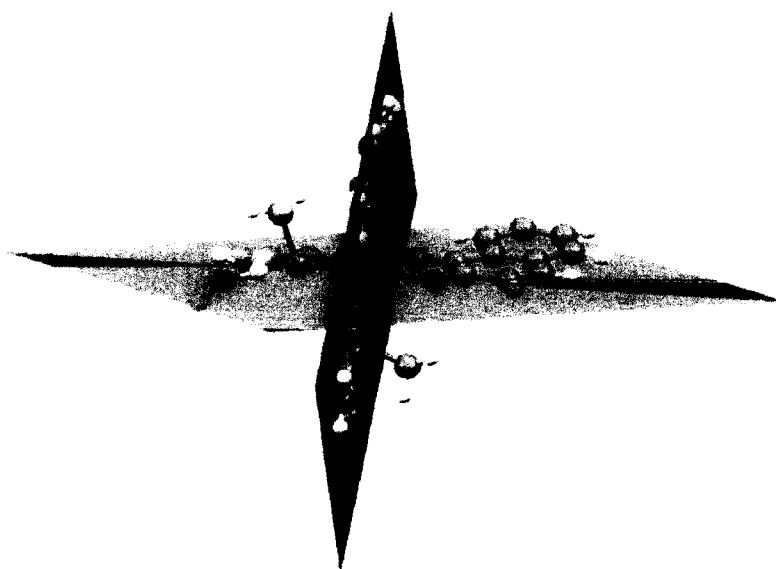


Figure V.2. Molecular view of the complex 11 showing two mutually perpendicular ligand units coordinated to ruthenium(II)

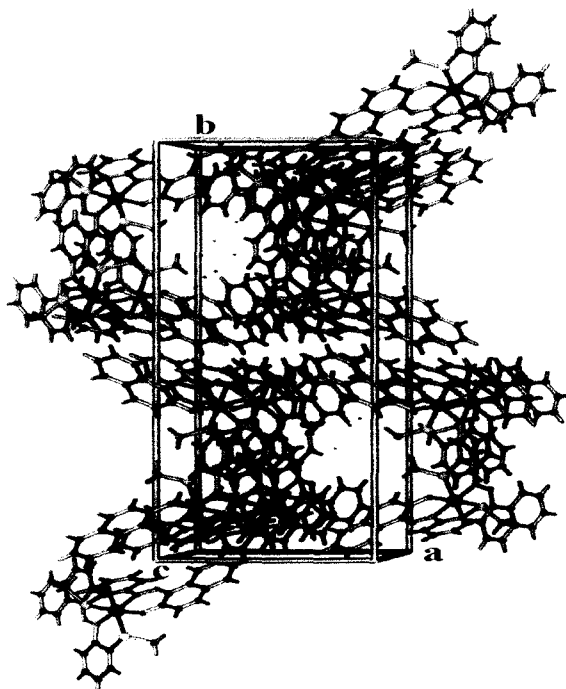
Table V.1. Crystal data and Structure Refinement Table

Empirical formula	C <sub>34</sub> H <sub>26</sub> Cl N <sub>4</sub> O <sub>2</sub> Ru S <sub>2</sub>
Formula weight	700.15
Temperature	293(2) K
Wavelength	0.71073 Å
Crystal system	Monoclinic
Space group	P21/c
Unit cell dimensions	$a = 11.963(5) \text{ \AA}$ $b = 31.523(13) \text{ \AA}$ $c = 8.976(4) \text{ \AA}$ $\alpha = 90^\circ$ $\beta = 104.021(7)^\circ$ $\gamma = 90^\circ$
Volume	3284(2) Å <sup>3</sup>
Z	4
Calculated density	1.416 Mg/m <sup>3</sup>
Absorption coefficient	0.659 mm <sup>-1</sup>
F(000)	1416
Crystal size	0.27 x 0.19 x 0.10 mm
Theta range for data collection	1.75° to 25.00°
Limiting indices	$-14 \leq h \leq 14$ $-37 \leq k \leq 37$ $-10 \leq l \leq 10$
Reflections collected	31590
Independent reflections	5790 [R(int) = 0.1153]
Absorption correction	multi-scan
Refinement method	Full-matrix least-squares on F <sup>2</sup>
Data / restraints / parameters	5790 / 0 / 420
Goodness-of-fit on F <sup>2</sup>	1.038
Final R indices [I>2sigma(I)]	R1 = 0.0736, wR2 = 0.2008
R indices (all data)	R1 = 0.1210, wR2 = 0.2295
Largest diff. peak and hole	1.259 and -0.656 e.Å <sup>-3</sup>

Table V. 2. Selected bond lengths (Å) and bond angles (°) for the complex **11**.

Bond lengths/ Å		Bond angles: °	
Ru(1)-N(2)	2.004(6)	N(2)-Ru(1)-N(4)	178.1(2)
Ru(1)-N(4)	2.018(6)	N(2)-Ru(1)-O(2)	86.6(2)
Ru(1)-O(2)	2.022(6)	N(4)-Ru(1)-O(2)	91.5(2)
Ru(1)-O(1)	2.029(5)	N(2)-Ru(1)-O(1)	92.2(2)
Ru(1)-S(1)	2.291(2)	N(4)-Ru(1)-O(1)	87.2(2)
Ru(1)-S(2)	2.294(2)	O(2)-Ru(1)-O(1)	86.7(2)
N(1)-N(2)	1.270(8)	N(2)-Ru(1)-S(1)	85.37(19)
N(3)-N(4)	1.286(8)	N(4)-Ru(1)-S(1)	95.27(18)
		O(2)-Ru(1)-S(1)	92.99(18)
		O(1)-Ru(1)-S(1)	177.53(16)
		N(2)-Ru(1)-S(2)	96.28(19)
		N(4)-Ru(1)-S(2)	85.57(19)
		O(2)-Ru(1)-S(2)	177.03(16)
		O(1)-Ru(1)-S(2)	92.68(16)
		S(1)-Ru(1)-S(2)	87.77(10)

The packing diagram of **11** is presented in Figure V.3. The crystal structure reveals supramolecular assemblies with molecular components self organized by C-H... $\pi$  interactions. In particular, there are three C-H... $\pi$  interactions, C22-H22... Cg5, C22-H22... Cg6 and C30-H30... Cg5 [where Cg5 and Cg6 are the centroids of C1-C10 and C5-C9 rings at  $-1+x, y, z$  and  $x, y, -1+z$  respectively (Figure V.4).

Figure V.3. Packing arrangement in **11**

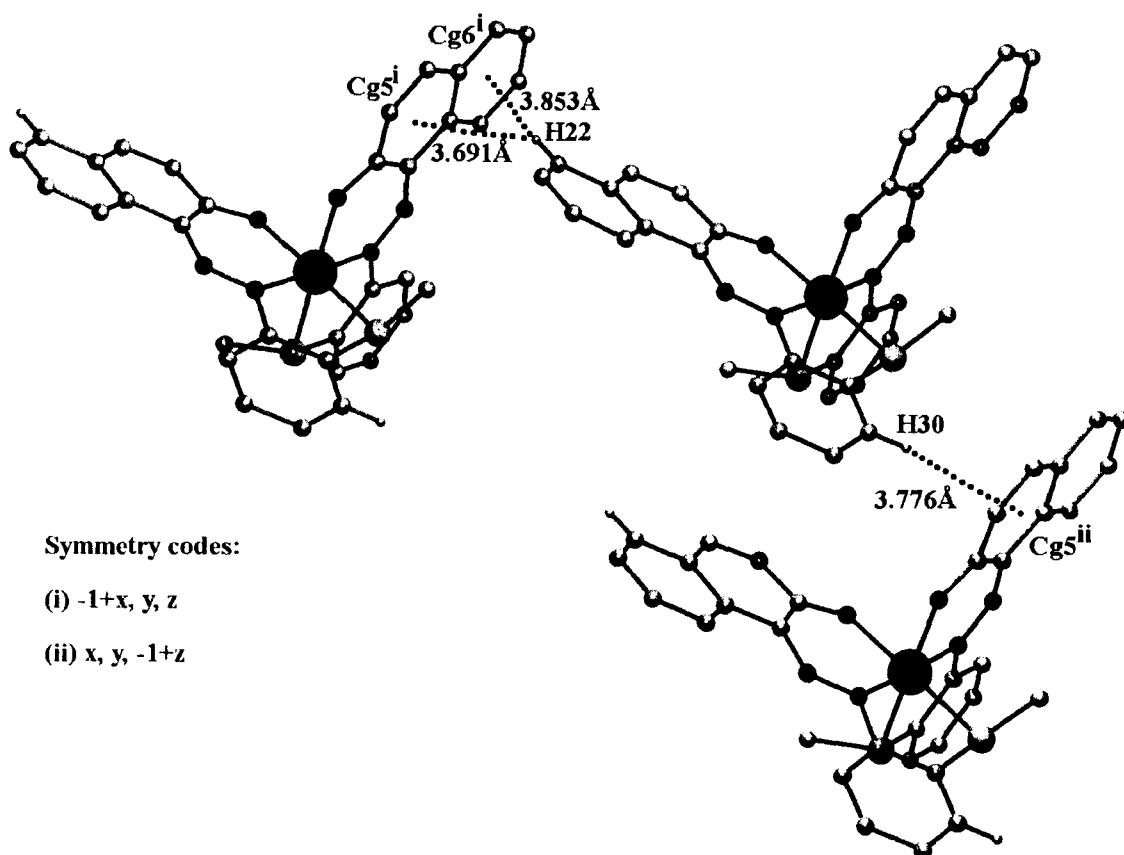


Figure V.4. Intermolecular C-H... $\pi$  interactions in **11**; Cg5 and Cg6 are the centroids of the rings C1-C10 & C5-C9 respectively.

## V. 2. 2 Spectral properties

### (a) IR Spectra

The infrared spectral data of the compounds are collected in solid state as KBr disc. As representative cases the infrared spectra of **(5)** and **(10)** are given in Figure V.5 and Figure V.6 respectively. The IR spectra of all the compounds show absorption in the range of  $1364-1370\text{ cm}^{-1}$  due to the presence of diazene ( $-N=N-$ ) group [10a]. The absorption in the range of  $3430\text{ cm}^{-1}$  which is due to the presence of  $-OH$  group, is absent in the IR spectra of all the compounds. Infrared spectra of all the complexes  $[Ru(PPh_3)_2(L)Cl]$  (1–10) show strong vibrations near  $518, 690$  and  $745\text{ cm}^{-1}$  which is attributed to *trans* –  $Ru(PPh_3)_2$  fragment [13, 14].

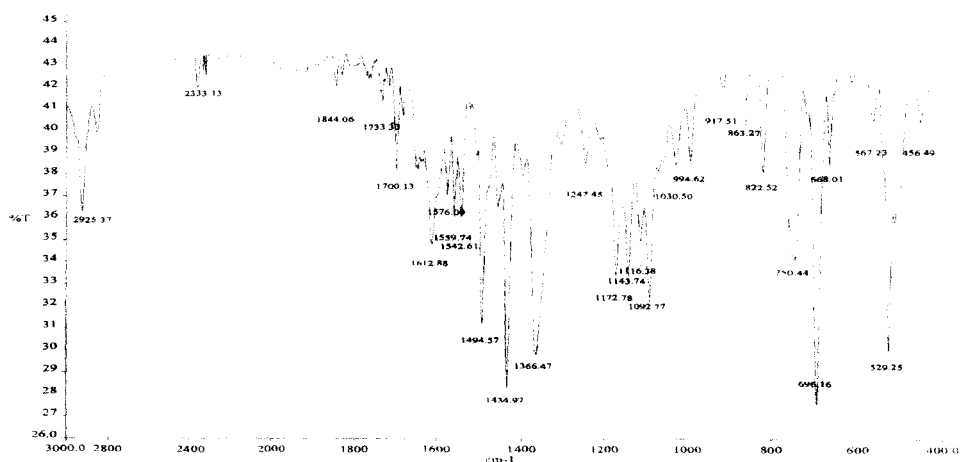


Figure V.5. IR-spectrum of compound (5) in KBr plate.

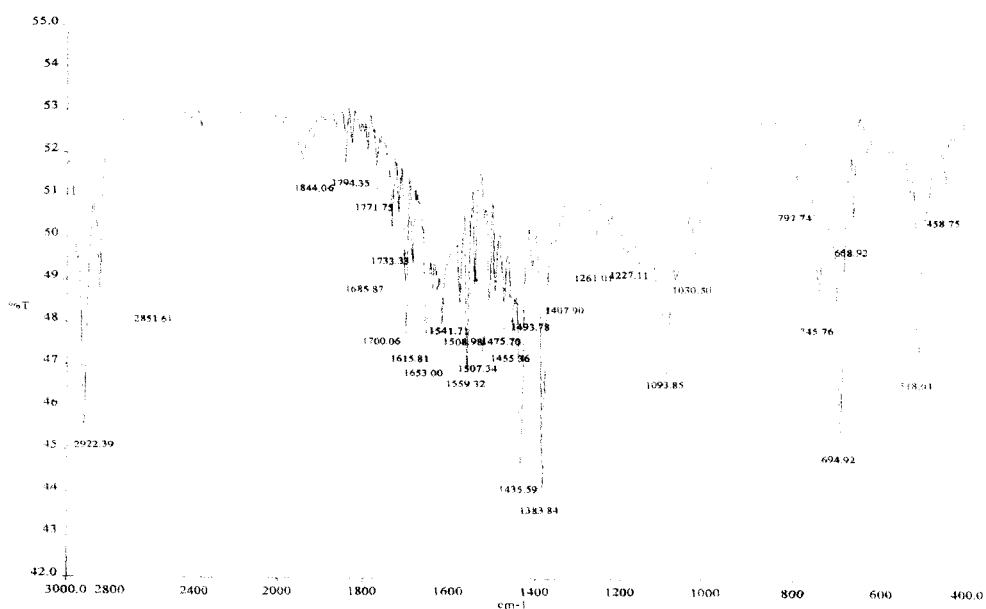


Figure V.6. IR-spectrum of compound (10) in KBr plate.

### (b) Electronic Spectra

The  $[\text{Ru}^{\text{II}}(\text{PPh}_3)_2(\text{L})\text{Cl}]$  (**1-10**) and  $[\text{Ru}^{\text{II}}(\text{L})_2]$  (**11-20**) compounds are soluble in polar organic solvents, such as chloroform, dichloromethane, acetone etc. and produce green colour. The electronic spectra were recorded in dichloromethane solution. Spectral data are presented in the Experimental Section. Electronic spectra of compounds (**11**), (**13**) and (**15**) are shown in Figure V.7. The electronic spectra of the compounds show one or more strong absorption in the visible region near 620, 420, 475 nm. This intense absorption is attributable to ligand to metal charge transfer (LMCT) transitions. The absorption in the ultraviolet region originates from the transition occurring within ligand to metal charge transfer (LMCT) transitions [7].

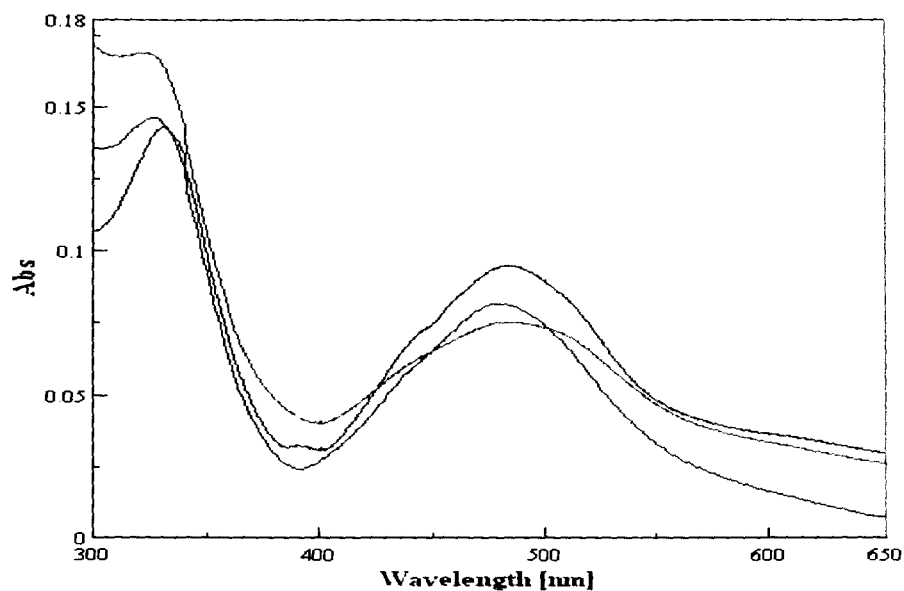


Figure V.7. Uv-vis spectra of **11** (Blue), **13** (Red), **15** (Green).

### (c) NMR Spectra

$^1\text{H}$  NMR spectra of the complexes have been recorded in  $\text{CDCl}_3$  Solution.  $^1\text{H}$  NMR spectral data of the compounds are given in experimental section. The selected  $^1\text{H}$  NMR spectra of the compounds (**2**) and (**6**) in  $\text{CDCl}_3$  have been displayed in Figure V.8 and Figure V.9 respectively. The aromatic region of the spectra ( $\delta$  7.0-8.0) appears a bit complex due to overlap of some signals and hence assignment of all the signals in this region to specific protons has not been possible. In  $^1\text{H}$  NMR spectra the signals for free -OH group was absent. However intensity measurements of the signals correspond to the total number of aromatic protons present in the respective complexes. In  $^1\text{H}$  NMR spectra the signals for -SCH<sub>3</sub> group of compound **1** and **6** appear as 2.9  $\delta$ . And that for -SCH<sub>2</sub> group of compound **5** and **10** appear at 3.54  $\delta$ .

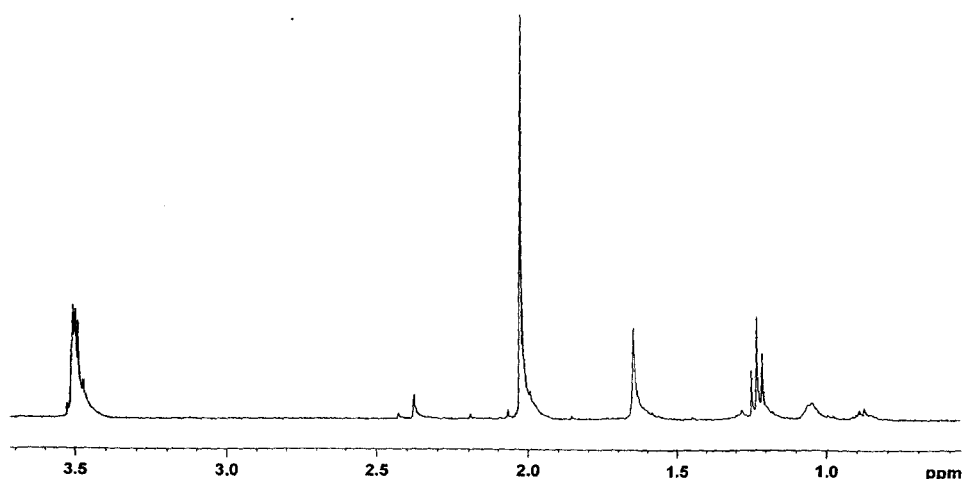


Figure V.8.  $^1\text{H}$  NMR spectrum of compound (**2**).

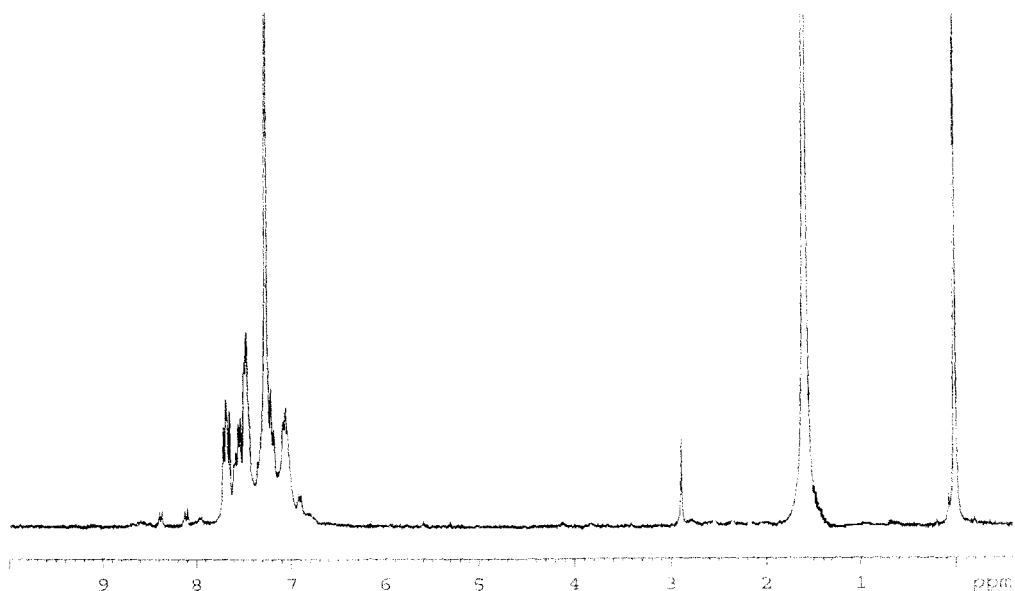


Figure V.9. <sup>1</sup>H NMR spectrum of compound (6).

### V. 2. 3. *UV-vis Spectra and Excited Singlet State Calculations*

The electronic spectra of all ruthenium(II) complexes (**1-20**) showed an allowed transition above 550 nm. Electronic spectra of azo-ruthenium(II) complexes invariably demonstrate similar patterns [3-10]. These transitions have been assigned to the metal-to-ligand charge-transfer (MLCT) transitions, Ru ( $t_2$ )  $\rightarrow$   $\pi^*$  (azo-ligand) within the framework of pseudo-octahedral ruthenium(II) stereochemistry [3,4]. To confirm the nature of the absorptions we proceeded to perform the time-dependent DFT (TD-DFT) calculations of the representative ruthenium(II) complex, **11** in dichloromethane. The coordinates of **11** has been directly imported from their crystal data. It is well known that an experimentally used model of an excited state corresponds to excitation of an electron from an occupied orbital to a virtual orbital. Assignment of the character of each excited states are based on the compositions of the occupied and virtual orbitals of the dominant configurations for that excited state. The TDDFT results do not provide information on triplet-singlet absorption intensities since spin-orbit coupling effects are not included in the current TDDFT methods. Thus we have only calculated the singlet excited states and only the singlet states with oscillator strengths greater than 0.05 are listed. The frontier molecular orbital compositions, excitation energies and oscillator strengths for the various absorption bands are reported in Table V.3 & V.4, together with the composition of the solution vectors in terms of most relevant transitions. The simulated spectrum of **11** has been presented in Figure V.10.

A detailed analysis of the highest occupied and lowest unoccupied molecular orbitals of **11** is presented in Table V.3, where orbital energies and composition in terms of atomic contributions are reported. In case of HOMO (107a), the largest orbital contributions arise from the ruthenium  $t_2$  orbitals of ruthenium. HOMO-1 and HOMO-2 also show a sizeable Ru- $d$  character (36% & 50% respectively). The lowest unoccupied molecular orbital (108a) is mostly concentrated on the diazene fragments. The other LUMO's have predominant ligand character. Isodensity surface plot of the relevant MO's is presented in Figure V.11. The HOMO-LUMO gap is computed to be  $\sim 1.318$  eV.

Table V.3. Energies and Percentage Composition of the Lowest unoccupied and Highest Occupied Kohn-Sham Orbitals of **11** in Terms of Pd and the ligand fragment<sup>a</sup>

MO	occ	E(eV)	Ru	Ligand
113a	0	-1.586		83.89
112a	0	-1.646		82.33
111a	0	-1.722		85.86
110a	0	-1.810		94.66
109a	0	-2.914	3.89 ( $d_{x^2-y^2}$ ); 2.41( $d_{xy}$ ).	65.8
<b>108a</b>	0	-3.032	2.92 ( $d_{z^2}$ ).	75.96
<b>107a</b>	2	-4.350	18.29 ( $d_{x^2-y^2}$ ); 13.22 ( $d_{z^2}$ ); 6.66( $d_{xy}$ ); 6.64( $d_{xz}$ ).	29.70
106a	2	-4.744	22.00 ( $d_{z^2}$ ); 6.00 ( $d_{xy}$ ); 5.47 ( $d_{xz}$ ); 2.50( $d_{yz}$ ).	31.49
105a	2	-4.933	16.85( $d_{xy}$ ); 14.83 ( $d_{yz}$ ); 11.21 ( $d_{x^2-y^2}$ ); 7.63 ( $d_{z^2}$ ).	25.46
104a	2	-5.295	10.70 ( $d_{z^2}$ ); 2.78 ( $d_{xy}$ ); 1.82 ( $d_{xz}$ ); 1.69 ( $d_{yz}$ ).	49.75
103a	2	-5.563	18.03 ( $d_{x^2-y^2}$ ); 5.69 ( $d_{xz}$ ); 2.89 ( $d_{z^2}$ ).	42.41
102a	2	-5.709	4.03( $d_{z^2}$ ); 2.72 ( $d_{xz}$ ); 1.43( $d_{xy}$ ).	61.26

Bold characters are used for the HOMO (107a) and the LUMO (108a).

Table V.4. Selected list of vertical excitations computed at the TD-DFT/PW91/TZP level for **11**.

State	Energy (eV)	$\lambda_{cal}$ (nm)	$\lambda_{exp}$ (nm)	f	Composition
S <sub>3</sub>	1.9187	646	-	0.017	HOMO-1 $\rightarrow$ LUMO (62.7%) HOMO-2 $\rightarrow$ LUMO (10.8%)
S <sub>5</sub>	2.2064	561	545	0.167	HOMO-2 $\rightarrow$ LUMO (60.0%) HOMO-1 $\rightarrow$ LUMO+1 (31.5%)
S <sub>13</sub>	2.8008	442	477	0.054	HOMO-4 $\rightarrow$ LUMO (35.7%) HOMO $\rightarrow$ LUMO+5 (16.0%) HOMO-3 $\rightarrow$ LUMO+1 (14.2%)
S <sub>14</sub>	2.8124	440	420	0.031	HOMO-6 $\rightarrow$ LUMO (38.8%) HOMO-4 $\rightarrow$ LUMO+1 (23.5%) HOMO-5 $\rightarrow$ LUMO (14.4%)
S <sub>33</sub>	3.4914	355	-	0.048	HOMO $\rightarrow$ LUMO+7 (70.8%) HOMO-8 $\rightarrow$ LUMO+7 (9.1%)
S <sub>54</sub>	3.9354	315	-	0.041	HOMO-5 $\rightarrow$ LUMO+2 (29.8%) HOMO-2 $\rightarrow$ LUMO+6 (18.6%) HOMO-2 $\rightarrow$ LUMO+7 (10.2%)

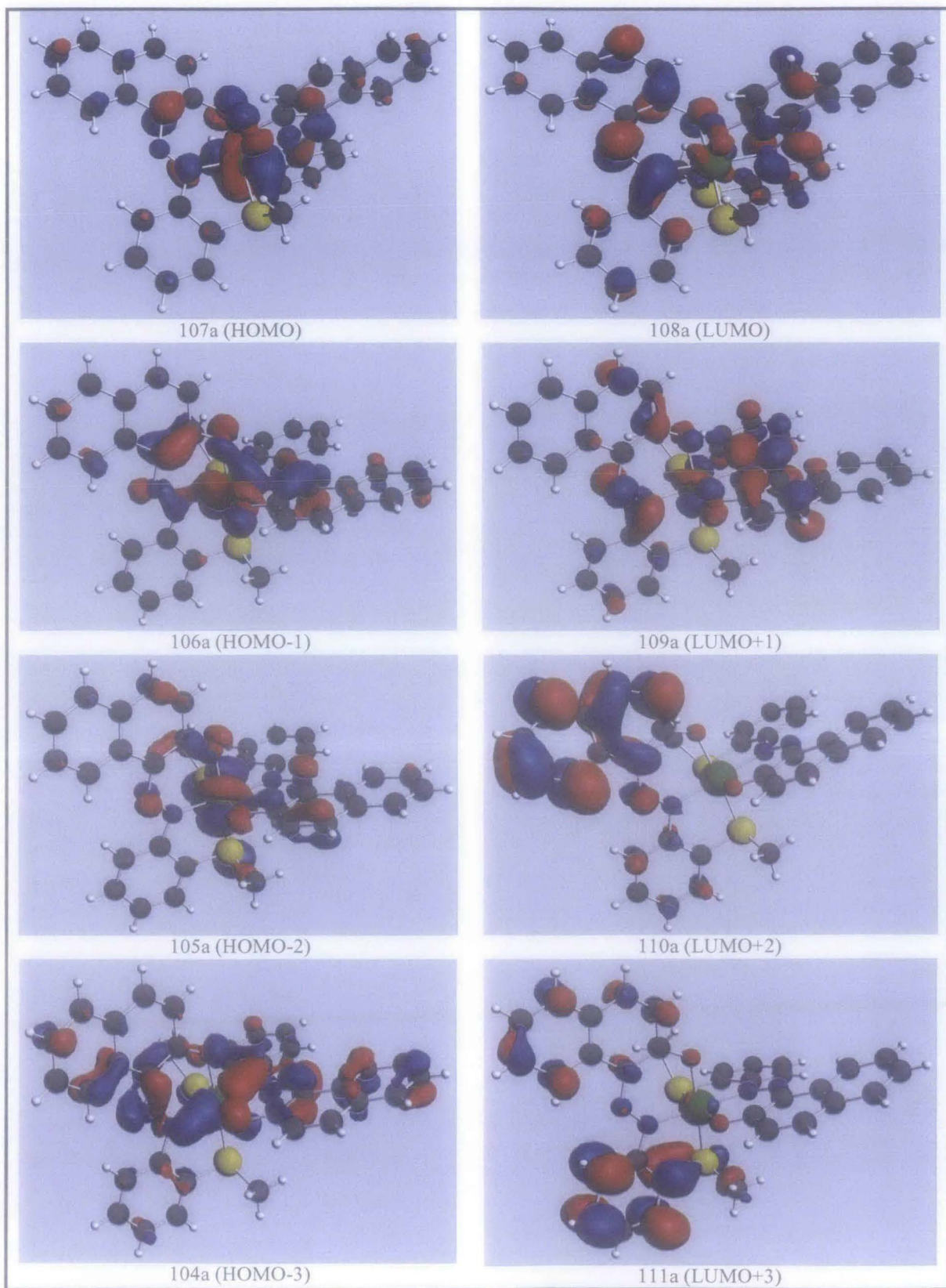


Figure V.11. DFT calculated frontier orbitals for complex 11.

The TDDFT computed transition energies in **11** at about 561 nm agree well with the observed band maxima at ca. 545 nm, suggesting the suitability of the calculations for these compounds. According to the calculations (Tables V.4), the intense transitions are from filled metal based  $t_2$  orbitals (HOMO-1 & HOMO-2) to the azo  $\pi^*$  unoccupied MOs, indicating a MLCT type transition. The other absorptions in the visible region in **11** have common density redistribution features with a significant amount of metal to ligand charge transfer and more or less  $\pi$ - $\pi^*$  intraligand density redistribution. The most intense transition observed in **11** in UV region (ca. 315 nm) involves excitation from 102a (HOMO-5) and 105a (HOMO-2) to 110a (LUMO+2) and 114a (LUMO-6) respectively with predominantly intraligand  $\pi$ - $\pi^*$  character (Table V.4). The computed electronic spectrum of the compound (**11**) is shown in Figure V.10.

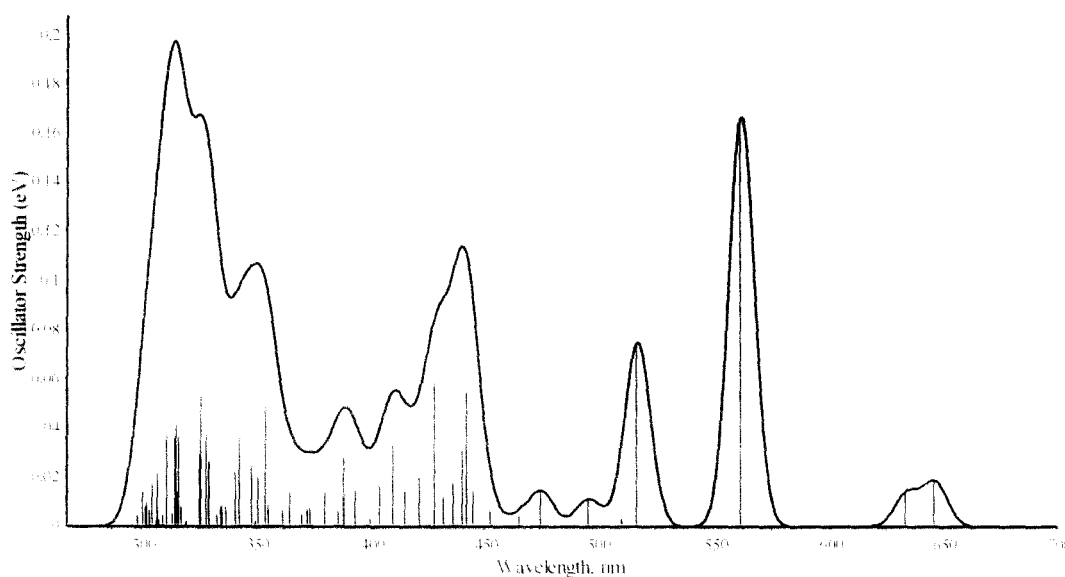


Figure V.10. Electronic spectrum computed at the TD-DFT/PW91/TZP level for **11**.

## V. 2. 4 Conclusions

1. Ruthenium(II) smoothly reacts with two groups of terdentate ligands *viz.* 2-hydroxy-1-(2'-alkylthiophenylazo)naphthalenes (HL<sup>1</sup>-HL<sup>5</sup>) and 1-hydroxy-2-(2'-alkylthiophenylazo)naphthalenes (HL<sup>6</sup>-HL<sup>10</sup>) and forms diamagnetic octahedral complexes with ONS coordination sphere. Two mutually trans triphenylphosphines and one axial chloride complete the coordination sphere.
2. The reaction between ruthenium trichloride (RuCl<sub>3</sub>, xH<sub>2</sub>O) and the diazene ligands afford diamagnetic octahedral ruthenium(II) complexes of the type [Ru<sup>II</sup>(L)<sub>2</sub>]. The two coordinated terdentate monoanionic ligands are almost perpendicular to each other.
3. The crystal structures of the representative complex confirm the octahedral coordination of ruthenium(II) with six-membered Ru-O-C-C-N-N chelate ring and five-membered Ru-N-C-C-S chelate ring.
4. Several intermolecular C-H... $\pi$  interactions have been found to stabilize the crystal packing in the ruthenium(II) complex.
5. The simulated electronic spectra of the ruthenium(II) complexes using time-dependent density functional theory (TD-DFT) are in close agreement with the experimental spectra.
6. The low energy absorptions have been attributed to metal-to-ligand charge transfer (MLCT) transitions originating from Ru-based orbitals to  $\pi^*$  (diazene). Whereas the high energy absorptions are due to intraligand  $\pi$ - $\pi^*$  transitions having a small admixture of MLCT transitions.

## V. 3 Experimental

### V. 3. 1 Preparation of compounds

#### a. Chemicals

Commercial Ruthenium trichloride, procured from Arora Matthey Ltd. Kolkata, India was dissolved in conc HCl and evaporated to dryness. The process was repeated thrice before use. Triphenylphosphine was procured from SD Fine chemicals, India. Complex [Ru(PPh<sub>3</sub>)<sub>3</sub>Cl<sub>2</sub>] was prepared by the method reported in literature [15]. Silica gel, benzyl chlorides were purchased from SD fine chemicals, India. 2-aminothiophenol, (Merck, Germany), 1-naphthol and 2-naphthol (E.Merck, India) were used without further purification. All solvents were purified according to standard procedure.

## ***b. Syntheses of the ligands***

2-hydroxy-1-(2'-alkylthiophenylazo)naphthalenes (HL<sup>1</sup>-HL<sup>5</sup>) and 1-hydroxy-2-(2'-alkylthiophenylazo)naphthalenes (HL<sup>6</sup>-HL<sup>10</sup>) were prepared following reported procedure using 2-naphthol and 1-naphthol respectively [16]. Detailed synthetic procedure and characterisation of the ligands have been outlined in Chapter II.

## ***c. Synthesis of complexe***

### *Preparation of [Ru(PPh<sub>3</sub>)<sub>3</sub>Cl<sub>2</sub>]*

Compound [Ru(PPh<sub>3</sub>)<sub>3</sub>Cl<sub>2</sub>] was prepared by the method reported in literature [15]. A mixture of commercially available ruthenium trichloride trihydrate (RuCl<sub>3</sub> · 3H<sub>2</sub>O), (2g) and concentrated HCl (10cm<sup>3</sup>) was taken in a porcelain basin and evaporated to dryness. The process was repeated thrice. The dark brown mass was dried in vacuo in presence of KOH. Ruthenium trichloride (0.4g) in methanol (50cm<sup>3</sup>) was taken in a three necked round bottomed flask fitted with a condenser and dinitrogen was slowly purged through the solution. Freshly recrystallized triphenylphosphine (2.4g) was added to the above solution and refluxed under dinitrogen atmosphere for 3h. Brown solid mass deposited. The solution was cooled and filtered. The precipitate was washed with methanol followed by diethyl ether. The compound was dried in vacuo.

## ***d. Isolation of compounds***

### *Isolation of [Ru<sup>II</sup>L<sup>I</sup>(PPh<sub>3</sub>)<sub>2</sub>Cl](1)*

Solid 2-hydroxy-1-(2'-methylthiophenylazo)naphthalene (HL<sup>1</sup>) (0.03g, 0.1 mmol) in ethanol (35cm<sup>3</sup>) was taken in a three necked round bottomed flask fitted with a condenser and dinitrogen was slowly purged through the solution for 15 min. Then a suspension of [Ru<sup>II</sup>(PPh<sub>3</sub>)<sub>3</sub>Cl<sub>2</sub>] (0.1g, 0.1mmol) in ethanol was added to the above solution and the reaction mixture was refluxed under dinitrogen atmosphere for 8h. The colour of the solution changed to dark green. The solution was cooled and light green solid started to deposit. The solid mass was filtered, dissolved in dichloromethane and evaporated to dryness. Then it was subjected to purification by thin layer chromatography on a silica plate with 30% ethyl acetate in petroleum ether as eluant. A dirty green band containing the compound (1) was obtained, which was extracted with acetone. Evaporation of this extract afforded green, analytically pure compound.

(Yield: 0.035g, 0.037 mmol, 37%). Anal. calc. for C<sub>33</sub>H<sub>43</sub>N<sub>2</sub>OSCIP<sub>2</sub>Ru: C, 66.7%; H, 4.5%; N, 2.9%. Found : C, 66.2%; H, 4%; N, 2.2%. IR (KBr: ν·cm<sup>-1</sup>): 1364(N = N), 529, 695, and 748 (coordinated PPh<sub>3</sub> ligands). UV-Vis (CH<sub>2</sub>Cl<sub>2</sub>), λ·nm (ε·dm<sup>3</sup>·mol<sup>-1</sup>·cm<sup>-1</sup>)

$^1$ ): 427 (7700), 477 (6300), 620 (2500).  $^1\text{H}$  NMR in  $\text{CDCl}_3$  (ppm): 2.9 (s, 3H,  $-\text{SCH}_3$ ), 6.7 – 8.8 (Other aromatic protons).

#### *Isolation of $[\text{Ru}^{\text{II}}\text{L}^2(\text{PPh}_3)_2\text{Cl}](2)$*

The synthesis of the compound (2) was done following the same method as described for compound (1). The amount of  $\text{HL}^2$  and  $[\text{Ru}(\text{PPh}_3)_3\text{Cl}_2]$  used were (0.031g, 0.1 mmol) and (0.1g, 0.1 mmol) respectively.

(Yield: 0.038g, 0.039 mmol, 39%). Anal.calc. for  $\text{C}_{54}\text{H}_{45}\text{N}_2\text{OSCIP}_2\text{Ru}$ : C, 67%; H, 4.7%; N, 2.9%. Found : C, 66.5%; H, 4.2%; N, 2.3%. IR (KBr;  $\nu/\text{cm}^{-1}$ ): 1365(N = N), 540, 696, and 722 (coordinated  $\text{PPh}_3$  ligands). UV/Vis ( $\text{CH}_2\text{Cl}_2$ ),  $\lambda/\text{nm}$  ( $\epsilon/\text{dm}^3 \text{mol}^{-1} \text{cm}^{-1}$ ): 427 (8500), 477 (7200), 620 (3400).  $^1\text{H}$  NMR in  $\text{CDCl}_3$  (ppm): 3.5 (m, 2H,  $-\text{SCH}_2$ ), 1.24 (t, 3H,  $-\text{CH}_3$ ), 6.7 – 8.8 (Other aromatic protons).

#### *Isolation of $[\text{Ru}^{\text{II}}\text{L}^3(\text{PPh}_3)_2\text{Cl}](3)$*

The preparation and isolation of  $[\text{Ru}^{\text{II}}\text{L}^3(\text{PPh}_3)_2\text{Cl}](3)$  was made following the above procedure. The following yield is based on  $\text{HL}^3$  (0.032g, 0.1mmol) and  $[\text{Ru}^{\text{II}}(\text{PPh}_3)_3\text{Cl}_2]$  (0.1g, 0.1 mmol).

(Yield: 0.035g, 0.036 mmol, 36%). Anal.calc. for  $\text{C}_{55}\text{H}_{47}\text{N}_2\text{OSCl P}_2\text{Ru}$ : C, 67.2%; H, 4.8%; N, 2.9%. Found : C, 66.9%; H, 4.2%; N, 2.5%. IR (KBr;  $\nu/\text{cm}^{-1}$ ): 1364(N = N), 541, 696, and 722 (coordinated  $\text{PPh}_3$  ligands). UV/Vis ( $\text{CH}_2\text{Cl}_2$ ),  $\lambda/\text{nm}$  ( $\epsilon/\text{dm}^3 \text{mol}^{-1} \text{cm}^{-1}$ ): 425 (10300), 477 (9100), 620 (3900).  $^1\text{H}$  NMR in  $\text{CDCl}_3$  (ppm): 3.4 (m, 2H,  $-\text{SCH}_2$ ), 1.62 (m, 2H,  $-\text{CH}_2$ ), 1.21 (t, 3H,  $-\text{CH}_3$ ), 6.7 – 8.8 (Other aromatic protons).

#### *Isolation of $[\text{Ru}^{\text{II}}\text{L}^4(\text{PPh}_3)_2\text{Cl}](4)$*

The preparation and isolation of  $[\text{Ru}^{\text{II}}\text{L}^4(\text{PPh}_3)_2\text{Cl}](4)$  was made following the above procedure. The following yield is based on  $\text{HL}^4$  (0.034g, 0.1 mmol) and  $[\text{Ru}^{\text{II}}(\text{PPh}_3)_3\text{Cl}_2]$  (0.1g, 0.1 mmol).

(Yield: 0.039g, 0.039 mmol, 39%). Anal.calc. for  $\text{C}_{56}\text{H}_{49}\text{N}_2\text{OSCl P}_2\text{Ru}$ : C, 67.5%; H, 4.9%; N, 2.8%. Found : C, 67.1%; H, 4.2%; N, 2.3%. IR (KBr;  $\nu/\text{cm}^{-1}$ ): 1364(N = N), 530, 695, and 748(coordinated  $\text{PPh}_3$  ligands). UV/Vis ( $\text{CH}_2\text{Cl}_2$ ),  $\lambda/\text{nm}$  ( $\epsilon/\text{dm}^3 \text{mol}^{-1} \text{cm}^{-1}$ ): 426 (11500), 475 (9700), 615 (4300).  $^1\text{H}$  NMR in  $\text{CDCl}_3$  (ppm): 3.48 (m, 2H,  $-\text{SCH}_2$ ), 1.61 (m, 2H,  $-\text{CH}_2$ ), 1.22 (m, 2H,  $-\text{CH}_2$ ), 0.88 (m, 3H,  $-\text{CH}_3$ ), 6.7 – 8.8 (Other aromatic protons).

#### *Isolation of $[\text{Ru}^{\text{II}}\text{L}^5(\text{PPh}_3)_2\text{Cl}](5)$*

The synthesis of the compound (5) was done following the same method as described for compound (1). The amount of  $\text{HL}^5$  and  $[\text{Ru}^{\text{II}}(\text{PPh}_3)_3\text{Cl}_2]$  used were (0.37g, 0.1 mmol) and (0.1g, 0.1 mmol) respectively.

(Yield: 0.33g, 0.032 mmol, 32%). Anal. calc. for  $C_{59}H_{47}N_2OSCl P_2Ru$ : C, 68.8%; H, 4.6%; N, 2.7%. Found : C, 68.2%; H, 4.1%; N, 2.2%. IR (KBr;  $\nu/cm^{-1}$ ): 1366(N = N), 529, 696, and 750 (coordinated  $PPh_3$  ligands). UV/Vis ( $CH_2Cl_2$ ),  $\lambda/nm$  ( $\epsilon/dm^3 mol^{-1} cm^{-1}$ ): 427 (13500), 476 (11600), 627 (5100).  $^1H$  NMR in  $CDCl_3$  (ppm): 3.52 (m, 2H, -SCH<sub>2</sub>), 6.7 – 8.8 (Other aromatic protons).

*Isolation of  $[Ru^{II}L^6(PPh_3)_2Cl](6)$*

This complex was prepared and purified by following the procedure as described for compound (1) and the reflux time was 8h. The following yield is based on  $HL^6$  (0.015g, 0.05 mmol) and  $[Ru^{II}(PPh_3)_3Cl_2]$  (0.05g, 0.05 mmol).

(Yield: 0.017g, 0.018 mmol, 36%). Anal. calc. for  $C_{53}H_{43}N_2OSClP_2Ru$ : C, 66.7%; H, 4.5%; N, 2.9%. Found : C, 66.1%; H, 4.1%; N, 2.3%. IR (KBr;  $\nu/cm^{-1}$ ): 1366(N = N), 532, 695, and 721 (coordinated  $PPh_3$  ligands). UV/Vis ( $CH_2Cl_2$ ),  $\lambda/nm$  ( $\epsilon/dm^3 mol^{-1} cm^{-1}$ ): 328 (13700), 443 (7300), 627 (3300).  $^1H$  NMR in  $CDCl_3$  (ppm): 2.91 (s, 3H, -SCH<sub>3</sub>), 6.7 – 8.8 (Other aromatic protons).

*Isolation of  $[Ru^{II}L^7(PPh_3)_2Cl](7)$*

The preparation and isolation of  $[Ru^{II}L^7(PPh_3)_2Cl](7)$  was made following the procedure as described for compound (1) and the reflux time was 8h. The following yield is based on  $HL^7$  (0.015g, 0.05 mmol) and  $[Ru^{II}(PPh_3)_3Cl_2]$  (0.05g, 0.05 mmol).

(Yield : 0.017g, 0.018 mmol, 35%). Anal. calc. for  $C_{54}H_{45}N_2OSCl P_2Ru$ : C, 67%; H, 4.7%; N, 2.9%. Found : C, 66.7%; H, 4.1%; N, 2.2%. IR (KBr;  $\nu/cm^{-1}$ ): 1365(N = N), 530, 692, and 722 (coordinated  $PPh_3$  ligands). UV/Vis ( $CH_2Cl_2$ ),  $\lambda/nm$  ( $\epsilon/dm^3 mol^{-1} cm^{-1}$ ): 328 (15100), 441 (7300), 621 (3900).  $^1H$  NMR in  $CDCl_3$  (ppm): 3.5 (m, 2H, -SCH<sub>2</sub>), 1.24 (t, 3H, -CH<sub>3</sub>), 6.7 – 8.8 (Other aromatic protons).

*Isolation of  $[Ru^{II}L^8(PPh_3)_2Cl](8)$*

This complex was prepared and purified by following the procedure as described for compound (1) and the reflux time was 8h. The following yield is based on  $HL^8$  (0.016g, 0.05 mmol) and  $[Ru^{II}(PPh_3)_3Cl_2]$  (0.05g, 0.05 mmol).

(Yield: 0.018g, 0.018 mmol, 36%). Anal. calc. for  $C_{55}H_{47}N_2OSCl P_2Ru$ : C, 67.2%; H, 4.8%; N, 2.9%. Found : C, 66.7%; H, 4.1%; N, 2.2%. IR (KBr;  $\nu/cm^{-1}$ ): 1365(N = N), 532, 696, and 721 (coordinated  $PPh_3$  ligands). UV/Vis ( $CH_2Cl_2$ ),  $\lambda/nm$  ( $\epsilon/dm^3 mol^{-1} cm^{-1}$ ): 326 (17300), 441(8100), 620 (4300).  $^1H$  NMR in  $CDCl_3$  (ppm): 3.4 (m, 2H, -SCH<sub>2</sub>), 1.61 (m, 2H, -CH<sub>2</sub>), 1.22 (t, 3H, -CH<sub>3</sub>), 6.7 – 8.8 (Other aromatic protons).

*Isolation of  $[Ru^{II}L^9(PPh_3)_2Cl](9)$*

The preparation and isolation of  $[\text{Ru}^{\text{II}}\text{L}^9(\text{PPh}_3)_2\text{Cl}](9)$  was made following the procedure as described for compound (1) and the reflux time was 8h. The following yield is based on  $\text{HL}^9$  (0.017g, 0.05 mmol) and  $[\text{Ru}^{\text{II}}(\text{PPh}_3)_3\text{Cl}_2]$  (0.05g, 0.05 mmol).

(Yield: 0.018g, 0.0185 mmol, 37%). Anal. calc. for  $\text{C}_{56}\text{H}_{49}\text{N}_2\text{OSCl P}_2\text{Ru}$ : C, 67.5%; H, 4.9%; N, 2.8%. Found : C, 67.2%; H, 4.3%; N, 2.2%. IR (KBr;  $\nu/\text{cm}^{-1}$ ): 1367(N = N), 530, 694, and 722 (coordinated  $\text{PPh}_3$  ligands). UV/Vis ( $\text{CH}_2\text{Cl}_2$ ),  $\lambda/\text{nm}$  ( $\epsilon/\text{dm}^3 \text{mol}^{-1} \text{cm}^{-1}$ ): 322 (17600), 443(9300), 620 (5600).  $^1\text{H}$  NMR in  $\text{CDCl}_3$  (ppm): 3.48 (m, 2H,  $-\text{SCH}_2$ ), 1.61 (m, 2H,  $-\text{CH}_2$ ), 1.24 (m, 2H,  $-\text{CH}_2$ ), 0.91 (m, 3H,  $-\text{CH}_3$ ), 6.7 – 8.8 (Other aromatic protons).

#### *Isolation of $[\text{Ru}^{\text{II}}\text{L}^{10}(\text{PPh}_3)_2\text{Cl}](10)$*

This complex was prepared and purified by following the procedure as described for compound (1) and the reflux time was 8h. The following yield is based on  $\text{HL}^{10}$  (0.019g, 0.05 mmol) and  $[\text{Ru}^{\text{II}}(\text{PPh}_3)_3\text{Cl}_2]$  (0.05g, 0.05 mmol).

(Yield: 0.016g, 0.016 mmol, 32%). Anal. calc. for  $\text{C}_{59}\text{H}_{47}\text{N}_2\text{OSCl P}_2\text{Ru}$ : C, 68.8%; H, 4.6%; N, 2.7%. Found : C, 68.3%; H, 4.2%; N, 2.1%. IR (KBr;  $\nu/\text{cm}^{-1}$ ): 1383(N = N), 518, 694, and 745 (coordinated  $\text{PPh}_3$  ligands). UV/Vis ( $\text{CH}_2\text{Cl}_2$ ),  $\lambda/\text{nm}$  ( $\epsilon/\text{dm}^3 \text{mol}^{-1} \text{cm}^{-1}$ ): 325 (27400), 440(12700), 620(6500).  $^1\text{H}$  NMR in  $\text{CDCl}_3$  (ppm): 3.54 (m, 2H,  $-\text{SCH}_2$ ), 6.7 – 8.8 (Other aromatic protons).

#### *Isolation of $[\text{Ru}^{\text{II}}(\text{L}^1)_2](11)$*

Solid 2-hydroxy-1-(2'-methylthiophenylazo)naphthalene ( $\text{HL}^1$ ) (0.03g, 0.1 mmol) in ethanol ( $35\text{cm}^3$ ) was taken in a three necked round bottomed flask fitted with a condenser and  $\text{NEt}_3$  (0.01g, 0.1mmol) was added to it. Dinitrogen was slowly purged through the solution for 15 min. Then a suspension of  $\text{RuCl}_3 \cdot 3\text{H}_2\text{O}$  (0.014g, 0.05mmol) in ethanol was added to the above solution and the reaction mixture was refluxed under dinitrogen atmosphere for 6h. The colour of the solution changed to brown. The solution was cooled and evaporated to dryness. The solid mass was dissolved in dichloromethane and subjected to purification by thin layer chromatography on a silica plate with 10% ethyl acetate in petroleum ether as eluant. A deep violet band containing the compound (11) was obtained, which was extracted with methanol. Evaporation of this extract afforded green, analytically pure compound.

(Yield: 0.02g, 0.029 mmol, 29%). Anal. calc. for  $\text{C}_{34}\text{H}_{26}\text{N}_4\text{O}_2\text{S}_2\text{Ru}$ : C, 59.4%; H, 3.8%; N, 8.2%. Found : C, 59.1%; H, 3.5%; N, 7.9%. IR (KBr;  $\nu/\text{cm}^{-1}$ ): 1365(N = N). UV/Vis ( $\text{CH}_2\text{Cl}_2$ ),  $\lambda/\text{nm}$  ( $\epsilon/\text{dm}^3 \text{mol}^{-1} \text{cm}^{-1}$ ): 429 (1200), 477 (1400), 535 (3800). *Isolation of  $[\text{Ru}^{\text{II}}(\text{L}^2)_2](12)$*

The synthesis of the compound (12) was done following the same method as described for compound (11). The amount of HL<sup>2</sup> and RuCl<sub>3</sub> · 3H<sub>2</sub>O used were (0.031g, 0.1 mmol) and (0.014g, 0.05 mmol) respectively.

(Yield: 0.022g, 0.031 mmol, 31%). Anal.calc. for C<sub>36</sub>H<sub>30</sub>N<sub>4</sub>O<sub>2</sub>S<sub>2</sub>Ru: C, 60.4%; H, 4.2%; N, 7.8%. Found : C, 60.1%; H, 3.9%; N, 7.6%. IR (KBr;  $\nu/\text{cm}^{-1}$ ): 1364(N = N). UV/Vis (CH<sub>2</sub>Cl<sub>2</sub>),  $\lambda/\text{nm}$  ( $\epsilon/\text{dm}^3 \text{ mol}^{-1} \text{ cm}^{-1}$ ): 420 (1500), 427 (1800), 542 (4300).

#### *Isolation of [Ru<sup>II</sup>(L<sup>3</sup>)<sub>2</sub>] (13)*

The synthesis of the compound (13) was done following the same method as described for compound (11). The amount of HL<sup>3</sup> and RuCl<sub>3</sub> · 3H<sub>2</sub>O used were (0.033g, 0.1 mmol) and (0.014g, 0.05 mmol) respectively.

(Yield: 0.025g, 0.034 mmol, 34%). Anal.calc. for C<sub>38</sub>H<sub>34</sub>N<sub>4</sub>O<sub>2</sub>S<sub>2</sub>Ru: C, 61.4%; H, 4.6%; N, 7.5%. Found : C, 61.1%; H, 4.2%; N, 7.2%. IR (KBr;  $\nu/\text{cm}^{-1}$ ): 1365(N = N). UV/Vis (CH<sub>2</sub>Cl<sub>2</sub>),  $\lambda/\text{nm}$  ( $\epsilon/\text{dm}^3 \text{ mol}^{-1} \text{ cm}^{-1}$ ): 421 (1900), 474 (2000), 545 (4800).

#### *Isolation of [Ru<sup>II</sup>(L<sup>4</sup>)<sub>2</sub>] (14)*

The synthesis of the compound (14) was done following the same method as described for compound (11). The amount of HL<sup>4</sup> and RuCl<sub>3</sub> · 3H<sub>2</sub>O used were (0.034g, 0.1 mmol) and (0.014g, 0.05 mmol) respectively.

(Yield: 0.023g, 0.03 mmol, 30%). Anal.calc. for C<sub>40</sub>H<sub>38</sub>N<sub>4</sub>O<sub>2</sub>S<sub>2</sub>Ru: C, 62.3%; H, 4.9%; N, 7.3%. Found : C, 62%; H, 4.5%; N, 7.1%. IR (KBr;  $\nu/\text{cm}^{-1}$ ): 1367(N = N). UV/Vis (CH<sub>2</sub>Cl<sub>2</sub>),  $\lambda/\text{nm}$  ( $\epsilon/\text{dm}^3 \text{ mol}^{-1} \text{ cm}^{-1}$ ): 418 (1600), 474 (2300), 554 (5100).

#### *Isolation of [Ru<sup>II</sup>(L<sup>5</sup>)<sub>2</sub>] (15)*

The synthesis of the compound (15) was done following the same method as described for compound (11). The amount of HL<sup>5</sup> and RuCl<sub>3</sub> · 3H<sub>2</sub>O used were (0.037g, 0.1 mmol) and (0.014g, 0.05 mmol) respectively.

(Yield: 0.023g, 0.028mmol, 28%). Anal.calc. for C<sub>46</sub>H<sub>34</sub>N<sub>4</sub>O<sub>2</sub>S<sub>2</sub>Ru: C, 65.8%; H, 4.1%; N, 6.7%. Found : C, 65.5%; H, 3.9%; N, 6.4%. IR (KBr;  $\nu/\text{cm}^{-1}$ ): 1364(N = N). UV/Vis (CH<sub>2</sub>Cl<sub>2</sub>),  $\lambda/\text{nm}$  ( $\epsilon/\text{dm}^3 \text{ mol}^{-1} \text{ cm}^{-1}$ ): 420 (2000), 476 (2700), 545 (6100).

#### *Isolation of [Ru<sup>II</sup>(L<sup>6</sup>)<sub>2</sub>] (16)*

The synthesis of the compound (16) was done following the same method as described for compound (11). The amount of HL<sup>6</sup> and RuCl<sub>3</sub> · 3H<sub>2</sub>O used were (0.015g, 0.05 mmol) and (0.007g, 0.025 mmol) respectively.

(Yield: 0.01g, 0.015 mmol, 30 %). Anal.calc. for C<sub>34</sub>H<sub>26</sub>N<sub>4</sub>O<sub>2</sub>S<sub>2</sub>Ru: C, 59.4%; H, 3.8%; N, 8.2%. Found : C, 59.2%; H, 3.4%; N, 7.8%. IR (KBr;  $\nu/\text{cm}^{-1}$ ): 1365(N = N). UV/Vis (CH<sub>2</sub>Cl<sub>2</sub>),  $\lambda/\text{nm}$  ( $\epsilon/\text{dm}^3 \text{ mol}^{-1} \text{ cm}^{-1}$ ): 480 (5600), 327 (10100).

#### *Isolation of [Ru<sup>II</sup>(L<sup>7</sup>)<sub>2</sub>] (17)*

The preparation and isolation of [Ru<sup>II</sup>(L<sup>7</sup>)<sub>2</sub>] (17) was made following the procedure as described for compound (11). The following yield is based on HL<sup>7</sup> (0.016g, 0.05 mmol) and RuCl<sub>3</sub>, 3H<sub>2</sub>O used were (0.007g, 0.025 mmol).

(Yield: 0.009g, 0.013 mmol, 26%). Anal.calc. for C<sub>36</sub>H<sub>30</sub>N<sub>4</sub>O<sub>2</sub>S<sub>2</sub>Ru: C, 60.4%; H, 4.2%; N, 7.8%. Found : C, 60.2%; H, 3.9%; N, 7.5%. IR (KBr;  $\nu/\text{cm}^{-1}$ ): 1368(N = N). UV/Vis (CH<sub>2</sub>Cl<sub>2</sub>),  $\lambda/\text{nm}$  ( $\epsilon/\text{dm}^3 \text{mol}^{-1} \text{cm}^{-1}$ ): 482 (6100), 330 (11200).

#### *Isolation of [Ru<sup>II</sup>(L<sup>8</sup>)<sub>2</sub>] (18)*

The preparation and isolation of [Ru<sup>II</sup>(L<sup>8</sup>)<sub>2</sub>] (18) was made following the procedure as described for compound (11). The following yield is based on HL<sup>8</sup> (0.016g, 0.05 mmol) and RuCl<sub>3</sub>, 3H<sub>2</sub>O used were (0.007g, 0.025 mmol).

(Yield: 0.011g, 0.015 mmol, 30%). Anal.calc. for C<sub>38</sub>H<sub>34</sub>N<sub>4</sub>O<sub>2</sub>S<sub>2</sub>Ru: C, 61.4%; H, 4.6%; N, 7.5%. Found : C, 61.2%; H, 4.3%; N, 7.1%. IR (KBr;  $\nu/\text{cm}^{-1}$ ): 1367(N = N). UV/Vis (CH<sub>2</sub>Cl<sub>2</sub>),  $\lambda/\text{nm}$  ( $\epsilon/\text{dm}^3 \text{mol}^{-1} \text{cm}^{-1}$ ): 484 (6400), 331 (9700).

#### *Isolation of [Ru<sup>II</sup>(L<sup>9</sup>)<sub>2</sub>] (19)*

The preparation and isolation of [Ru<sup>II</sup>(L<sup>9</sup>)<sub>2</sub>] (19) was made following the procedure as described for compound (11). The following yield is based on HL<sup>9</sup> (0.017 g, 0.05 mmol) and RuCl<sub>3</sub>, 3H<sub>2</sub>O used were (0.007g, 0.025 mmol).

(Yield: 0.011g, 0.014mmol, 28 %). Anal.calc. for C<sub>40</sub>H<sub>38</sub>N<sub>4</sub>O<sub>2</sub>S<sub>2</sub>Ru: C, 62.3%; H, 4.9%; N, 7.3%. Found : C, 62%; H, 4.4%; N, 7%. IR (KBr;  $\nu/\text{cm}^{-1}$ ): 1364(N = N). UV/Vis (CH<sub>2</sub>Cl<sub>2</sub>),  $\lambda/\text{nm}$  ( $\epsilon/\text{dm}^3 \text{mol}^{-1} \text{cm}^{-1}$ ): 484 (6600), 327 (13500).

#### *Isolation of [Ru<sup>II</sup>(L<sup>10</sup>)<sub>2</sub>] (20)*

The synthesis of the compound (20) was done following the same method as described for compound (11). The amount of HL<sup>10</sup> and RuCl<sub>3</sub>, 3H<sub>2</sub>O used were (0.019g, 0.05 mmol) and (0.007g, 0.025 mmol) respectively.

(Yield: 0.0135g, 0.016mmol, 32%). Anal.calc. for C<sub>46</sub>H<sub>34</sub>N<sub>4</sub>O<sub>2</sub>S<sub>2</sub>Ru: C, 65.8%; H, 4.1%; N, 6.7%. Found : C, 65.6%; H, 3.8%; N, 6.3%. IR (KBr;  $\nu/\text{cm}^{-1}$ ): 1378(N = N). UV/Vis (CH<sub>2</sub>Cl<sub>2</sub>),  $\lambda/\text{nm}$  ( $\epsilon/\text{dm}^3 \text{mol}^{-1} \text{cm}^{-1}$ ): 484 (7000), 327 (15700).

### ***V. 3. 2 Characterization of the compounds***

All the ruthenium compounds were characterized by C, H and N microanalysis. The microanalytical data of all the compounds (Table.II.8) are in good agreement with the proposed composition

### ***V. 3. 3 Physical Measurements***

The IR spectra were obtained on a Jasco 5300 FT-IR spectrophotometer as KBr disks. Far-IR spectra were obtained from Bruker IFS-65 spectrophotometer. Electronic spectra were recorded on a Jasco V-500 spectrophotometer. <sup>1</sup>H NMR spectra were recorded on Bruker DPX 300 spectrometer. C, H and N elemental analysis were done by either Perkin-Elmer (Model 240C) or Hercus Carlo Erba 1108 elemental analyzer.

### ***V. 3. 4 Crystallography***

Single crystal of the ruthenium(II) complex (**11**) were grown by slow diffusion of a dichloromethane solution of the complexes into n-hexane. Crystallographic and refinement data for the reported structures are presented in Table VI.1 & Table VI.2. Other informations are described in Chapter II, Section II.3.3.

### ***V. 3. 5 Method and Computational Details***

Described in Chapter II, Section II.3.5

## References

1. (a) R. Drozdok, B. Allaert, N. Ledoux, I. Dragutan, V. Drgutan, F. Verpoort, *Coord Chem Rev.*, **249**, 3055 (2005); (b) M.K. Nazeeruddin, C. Klein, P. Liska, M. Gratzel, *Coord Chem. Rev.*, **249**, 1460 (2005); (c) J.K. Hurst, *Coord Chem Rev.*, **249**, 313 (2005); (d) I. Spiccia, G.B. Deacon, C.M. Kepert, *Coord Chem Rev.*, **248**, 1329 (2004); (e) B. Serli, E. Zangrando, T. Gianferrara, L. Yellowlers, E. Alersio E., *Coord. Chem Rev.*, **245**, 73 (2003); (f) V. Balzani, A. Juris, *Coord. Chem Rev.*, 211, 97 (2001).
2. (a) B.K. Ghosh, A. Chakravorty, *Coord. Chem Rev.*, **239**, 25 (1989); (b) E.A. Seddon, K.R. Seddon, *The Chemistry of Ruthenium*, Elsevier, Amsterdam (1984).
3. (a) A.R. Chakravarty, A. Chakravorty, F.A. Cotton, L.R. Falvello, B.K. Ghosh, T. Milagros, *Inorg. Chem.*, **22**, 1892 (1983); (b) B.K. Ghosh, A. Mukhopadhyay, S. Goswami, S. Ray, A. Chakravorty, *Inorg. Chem.*, **23**, 4633 (1984); (c) A. Seal, S. Ray, *Acta Crystallogr. Sect. C: Cryst. Struct. Commun.*, **C40**, 929 (1984).
4. (a) A.R. Chakravarty, A. Chakravorty, *Inorg. Chem.*, **20**, 275 (1981); (b) A.R. Chakravarty, A. Chakravorty, *Inorg. Chem.*, **20**, 3138 (1981); (c) A.R. Chakravarty, A. Chakravorty, *Inorg. Nucl., Chem. Lett.*, **15**, 307 (1979).
5. (a) R.K. Rath, M. Nethaji, A.R. Chakravorty, *J. Organomet. Chem.*, **633**, 79 (2001); (b) K. Sui, S.M. Peng, S. Bhattacharya, *Polyhedron*, **19**, 631 (1999).
6. F. Basuli, S.M. Peng, S. Bhattacharya, *Polyhedron*, **18**, 391 (1998).
7. P. Gupta, S. Dutta, F. Basuli, S.M. Peng, G.S. Lee, S. Bhattacharya, *Inorg. Chem.*, **45**, 460 (2006).
8. S. Goswami, R.N. Mukherjee, A. Chakravorty, *Inorg. Chem.*, **22**, 2825 (1983).
9. (a) S. Goswami, A.R. Chakravorty, A. Chakravorty, *Inorg Chem.*, **20**, 2246 (1981); (b) S. Goswami, A.R. Chakravorty, A. Chakravorty, *Inorg Chem.*, **21**, 2737 (1982); (c) S. Goswami, A.R. Chakravorty, A. Chakravorty, *Chem Soc, Chem Commun.*, 1288 (1982); (d) S. Goswami, A.R. Chakravorty, A. Chakravorty, *Inorg. Chem.*, **22**, 602 (1983); (e) P. Ghosh, A. Chakravorty, *J. Chem. Soc, Dalton Trans*, 361 (1985); (f) A.K. Mahapatra, B.K. Ghosh, S. Goswami, A. Charavorty, *J. Indian Chem Soc.*, **63**, 101 (1986).
10. (a) A.K. Mahapatra, S. Datta, S. Goswami, M. Mukherjee, A.K. Mukherjee, A. Chakravorty, *Inorg Chem.*, **25**, 1715 (1986); (b) A.K. Mukherjee, M. Mukherjee,

- P.K. Das, A.K. Mahapatra, S. Goswami, A. Chakravorty, *Acta Crystallogr. Sect C.: Cryst. Struct. Commun.*, **C42**, 793 (1986).
11. J. Chatt, J.M. Davidson, *J. Chem Soc.*, 843 (1965).
12. U.A. Gregory, S.D. Ibekwe, B.T. Kilbourn, D.R. Russell, *J. Chem., Soc. A*, 1118 (1971).
13. S. Bhattacharya, C.G. Piperpont, *Inorg. Chem.*, **30**, 2906 (1991).
14. A.K. Das, S.M. Peng, S. Bhattacharya, *J. Chem. Soc., Dalton Trans.*, 181 (2000).
15. T.A. Stephenson, G. Wilkinson, *J. Inorg. Nucl. Chem.*, **28**, 945 (1966).
16. (a) A. Burawoy, C. Turner, W.I. Hyslop, P. Raymakers, *J. Chem. Soc.*, 82 (1954);  
(b) A.I. Vogel, *A Text Book of Practical Organic Chemistry*, 3<sup>rd</sup> Ed., ELBS & Longman Group Ltd. (1971).